

The Nucleosynthesis of the Light Elements C to Al by Core Collapse Supernovae

Alessandro Chieffi^{1,3,4} and Marco Limongi^{2,3,4}

¹ Istituto di Astrofisica Spaziale e Fisica Cosmica (CNR), Via Fosso del Cavaliere, I-00133, Roma, Italy
achieffi@rm.iasf.cnr.it

² Istituto Nazionale di Astrofisica — Osservatorio Astronomico di Roma,
Via Frascati 33, I-00040, Monteporzio Catone, Italy
marco@mporzio.astro.it

³ School of Mathematical Sciences, PO Box 28M, Monash University, Victoria 3800, Australia

⁴ Centre for Astrophysics and Supercomputing, Swinburne University of Technology,
Mail Number 31, PO Box 218, Hawthorn, Victoria 3122, Australia

Received 2003 May 8, accepted 2003 June 1

Abstract: We discuss the production sites of the nuclei from C to Al in solar metallicity stars in the range 13–35 M_{\odot} . We will show how, contrary to current beliefs, the advanced burning phases and the passage of the blast wave play a pivotal role in determining the final yields of quite a few ‘light’ nuclei. We will also show how the relative contributions of the hydrostatic and explosive burning depend on the initial mass of the star: the smaller the mass the larger the importance of the explosive burning.

Keywords: nuclear reactions, nucleosynthesis, abundances — stars: evolution — stars: interiors — supernovae: general

1 Introduction

In a recent paper (Limongi & Chieffi 2003) we have presented a new set of solar metallicity models in the range 13–35 M_{\odot} . We have followed the hydrostatic evolution of each stellar model up to the beginning of the core collapse with FRANEC (Frascati RAPHSON Newton Evolutionary Code, version 4.97) and we have then shifted to a hydro code to follow the passage of the blast wave through the mantle of the models. We have discussed in that paper the global properties of the models, the explosions and the final yields. In this paper we discuss in more detail the production sites of the nuclei between C and Al. These nuclei are often thought to be the product of just the hydrostatic burning plus, at most, a contribution from the neutrino irradiation occurring during the explosion. Conversely we will show that there is a strong dependence of the production site and of the production events that lead to the synthesis (or destruction) of these ‘light’ nuclei on the initial mass of the star. A good knowledge of the history of each of these nuclei as a function of the initial mass is also important to understand how firmly their yields can be predicted at present. The set of models is the one already discussed in Limongi & Chieffi (2003) so that all the quantitative estimates of the yields may be found in that paper. All the comments related to the 15 M_{\odot} model apply to the 13 M_{\odot} model as well.

2 The Production of C and N

Figures 1, 2, and 3 show the final profiles of ^{12}C (thick solid line) and ^{13}C (thick dotted line) in panel (a) and of ^{14}N (thick solid line) and ^{15}N (thick dotted line) in panel (b) for the three model stars of 15, 25, and 35 M_{\odot} . The

thin solid, short dashed, and long dashed lines show, as a reference, the final profiles of ^4He , ^{16}O , and ^{20}Ne respectively. ^{12}C is produced in the central He burning via the 3α processes and partially destroyed towards the end of the central He burning by the $^{12}\text{C}(\alpha, \gamma)^{16}\text{O}$ reaction. C burning obviously depletes ^{12}C while burning outward in mass. Hence this isotope is confined, at the beginning of the core collapse, between the base of the last C convective shell and the border of the carbon–oxygen core. ^{13}C is produced at the beginning of the main sequence phase just outside the H convective core by a partial activation of the CN cycle (i.e. it is produced by the $^{12}\text{C}(\text{p}, \gamma)^{13}\text{N}(\beta^+)^{13}\text{C}$ process but is not yet destroyed by the $^{13}\text{C}(\text{p}, \gamma)^{14}\text{N}$ process) and then brought to the surface (and hence preserved) by the first dredge-up. ^{14}N is produced in the H convective core by the conversion of C and O in ^{14}N ; it is then partially brought into the convective envelope (and hence preserved) by the first dredge-up; ^{14}N is basically depleted by the He burning so that it is eventually preserved only outside the outer border of the He convective shell. ^{15}N is basically destroyed by the H burning so that the first dredge-up in this case leads to a net (small) reduction of the surface abundance of this isotope. The passage of the shock wave does not alter the final yields of these isotopes because they are abundant in regions too far (in radius) from the centre to be affected by the explosive burning; only ^{15}N may receive a contribution from the neutrino irradiation (Woosley & Weaver 1995; Rauscher et al. 2002).

3 The Production of O and F

Figures 1, 2, and 3 show the final profiles of ^{16}O (thick solid line), ^{17}O (thick dotted line), and ^{18}O (thick dashed

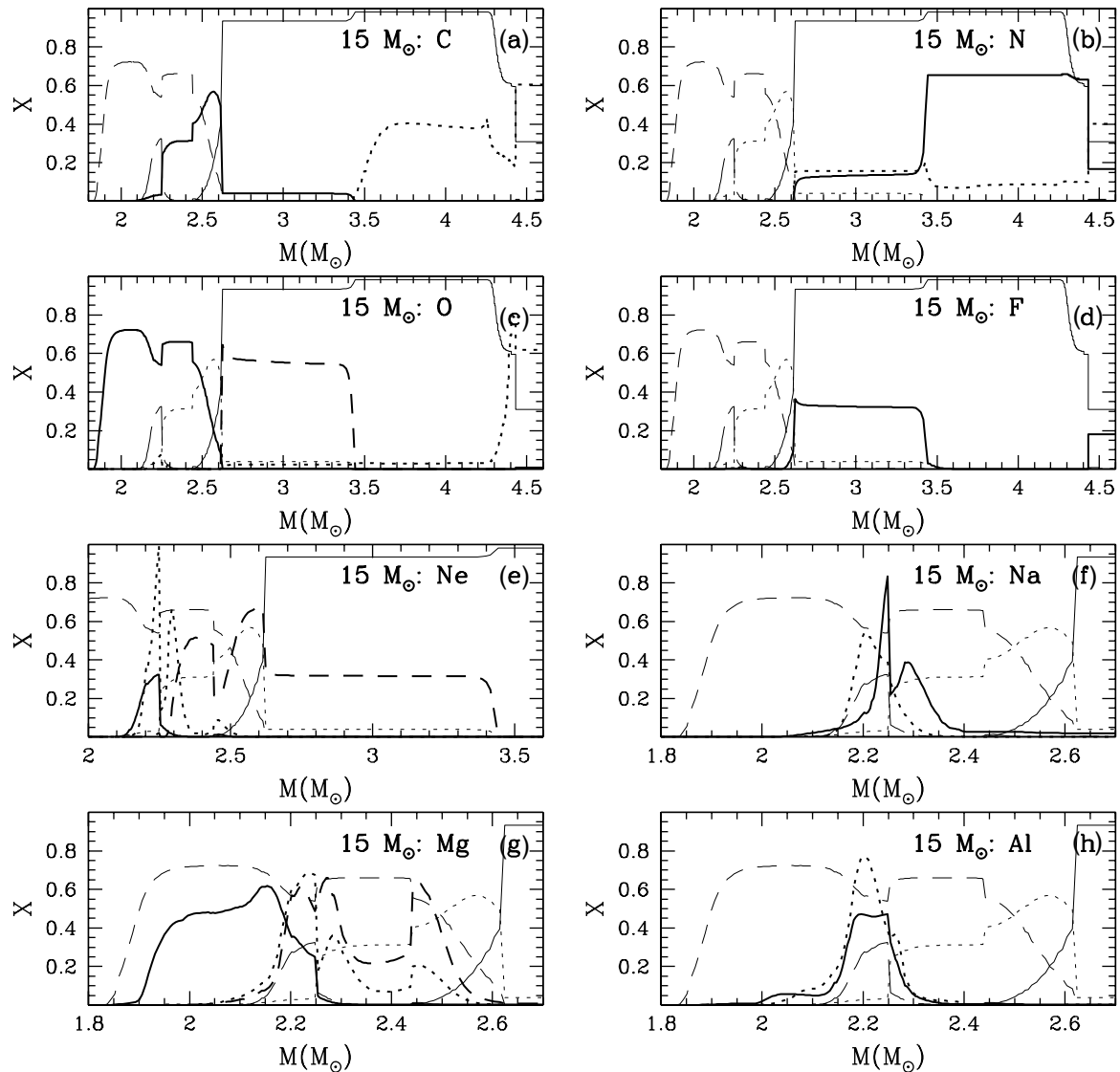


Figure 1 Profiles of the various isotopes at the beginning of the core collapse in the $15 M_{\odot}$ model. As a reference, the thin lines in all panels show the profiles of ${}^4\text{He}$ (solid), ${}^{12}\text{C}$ (dotted), ${}^{16}\text{O}$ (short dashed) and ${}^{20}\text{Ne}$ (long dashed). The thick lines in the eight panels refer to: panel (a) ${}^{12}\text{C}$ (solid), ${}^{13}\text{C}$ (dotted); panel (b) ${}^{14}\text{N}$ (solid), ${}^{15}\text{N}$ (dotted); panel (c) ${}^{16}\text{O}$ (solid), ${}^{17}\text{O}$ (dotted), ${}^{18}\text{O}$ (dashed); panel (d) ${}^{19}\text{F}$ (solid); panel (e) ${}^{20}\text{Ne}$ (solid), ${}^{21}\text{Ne}$ (dotted), ${}^{22}\text{Ne}$ (dashed); panel (f) ${}^{22}\text{Na}$ (dotted), ${}^{23}\text{Na}$ (solid); panel (g) ${}^{24}\text{Mg}$ (solid), ${}^{25}\text{Mg}$ (dotted), ${}^{26}\text{Mg}$ (dashed); panel (h) ${}^{26}\text{Al}$ (dotted), ${}^{27}\text{Al}$ (solid). To improve the readability of the figure the abundances of several isotopes have been rescaled (multiplied) by the following factors: ${}^{13}\text{C}$ (5×10^3), ${}^{14}\text{N}$ (50), ${}^{15}\text{N}$ (2×10^5), ${}^{17}\text{O}$ (5×10^4), ${}^{18}\text{O}$ (10^2), ${}^{19}\text{F}$ (2×10^5), ${}^{21}\text{Ne}$ (2×10^3), ${}^{22}\text{Ne}$ (2×10^5), ${}^{23}\text{Na}$ (50), ${}^{24}\text{Mg}$ (5), ${}^{25}\text{Mg}$ (50), ${}^{26}\text{Mg}$ (50), ${}^{26}\text{Al}$ (10^4), ${}^{27}\text{Al}$ (50).

line) in panel (c) and of ${}^{19}\text{F}$ (thick solid line) in panel (d) for the three model stars of 15, 25, and $35 M_{\odot}$. The thin solid, dotted, and dashed lines show, as a reference, the final profiles of ${}^4\text{He}$, ${}^{12}\text{C}$, and ${}^{20}\text{Ne}$ respectively. ${}^{16}\text{O}$ is the main product of the He burning so that its production depends on both the ${}^{12}\text{C}(\alpha, \gamma){}^{16}\text{O}$ cross section and the adopted mixing scheme. It is then destroyed by the advancing oxygen burning shell and then partly modified by the blast wave (destroyed by the explosive oxygen burning and rebuilt by the Ne explosive burning); this means that the determination of its final yield requires the computation of the full evolution of the star, including the passage of the blast wave. ${}^{17}\text{O}$ is mainly produced (and confined) at the outer border of the H convective core as a consequence of the combined effects of the CNO cycle

and the recession of the convective core itself. The first dredge-up brings this isotope into the convective envelope preserving it from destruction. ${}^{18}\text{O}$ is produced by the sequence ${}^{14}\text{N}(\alpha, \gamma){}^{18}\text{F}(\beta^+){}^{18}\text{O}$ and soon after destroyed by the reaction ${}^{18}\text{O}(\alpha, \gamma){}^{22}\text{Ne}$. The conversion of ${}^{14}\text{N}$ into ${}^{22}\text{Ne}$ closely follows the He ignition so that the ${}^{18}\text{O}$ may survive only in the He convective shell where the ${}^{14}\text{N}$ engulfed by the advancing convective shell has no time to be converted into ${}^{22}\text{Ne}$ because of the very short duration of the advanced nuclear burning. ${}^{19}\text{F}$ is largely destroyed in the H convective core by the ${}^{19}\text{F}(\text{p}, \alpha){}^{16}\text{O}$ reaction so that the surface abundance of this element slightly lowers at the end of the first dredge-up. At the beginning of the central He burning ${}^{19}\text{F}$ is produced by the sequence ${}^{18}\text{O}(\text{p}, \alpha){}^{15}\text{N}(\alpha, \gamma){}^{19}\text{F}$. The protons required to activate

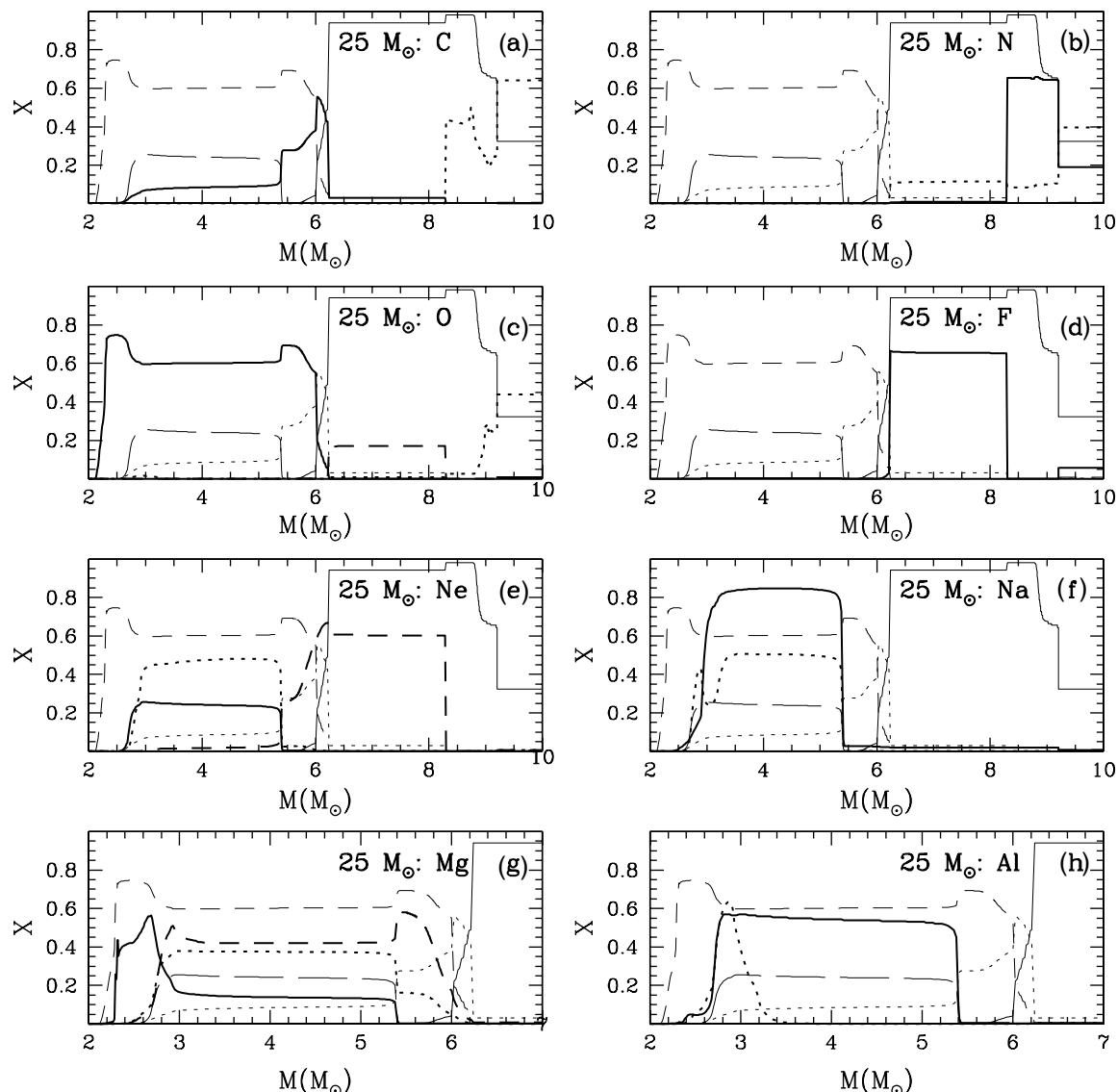


Figure 2 Same as Figure 1 but for the $25 M_{\odot}$ model.

this sequence are provided by the $^{14}\text{N}(n, p)^{14}\text{C}$ reaction that, in turn, is activated by the neutrons released by the $^{13}\text{C}(\alpha, n)^{16}\text{O}$ reaction. As the central He burning proceeds further on, ^{19}F is progressively destroyed by the reaction $^{19}\text{F}(\alpha, p)^{22}\text{Ne}$ and also the $^{19}\text{F}(p, \alpha)^{16}\text{O}$ process, so that all fluorine is destroyed in the He convective core at the central He exhaustion. Once the He convective shell forms, the same processes activate again so that the star reaches core collapse while fluorine is still increasing in the He convective shell. Since all the fluorine produced is confined in the He convective shell, the passage of the blast wave does not directly affect its abundance. It is worth noting, however, that Woosley & Weaver (1995) and Rauscher et al. (2002) showed that neutrino induced reactions may strongly enhance the fluorine yield.

4 The Production of Ne and Na

Figures 1, 2, and 3 show the final profiles of ^{20}Ne (thick solid line), ^{21}Ne (thick dotted line), and ^{22}Ne (thick dashed

line) in panel (e) and of ^{22}Na (thick dotted line) and ^{23}Na (thick solid line) in panel (f) for the three model stars of 15, 25, and $35 M_{\odot}$. The thin solid, dotted, and dashed lines show, as a reference, the final profiles of ^4He , ^{12}C , and ^{16}O respectively. Both ^{20}Ne and ^{21}Ne are produced by C burning and then destroyed by the successive Ne burning. Hence their production is confined, at the moment of the core collapse, to the C convective shell. Their final yields will therefore largely depend on the amount of C left by the He burning and also on the final location of the C convective shell. The influence of the passage of the shock wave on the final yields of these two nuclei depends on the initial mass of the star. In particular, in the $15 M_{\odot}$ model the pre-explosive abundances of ^{20}Ne and ^{21}Ne are destroyed by the passage of the shock wave and then synthesised again by the explosive C burning: Figure 1 shows clearly how the C convective shell has been largely reprocessed by the passage of the shock wave. As the initial mass of the star increases, the effect of the blast wave on these two nuclei reduces because the C

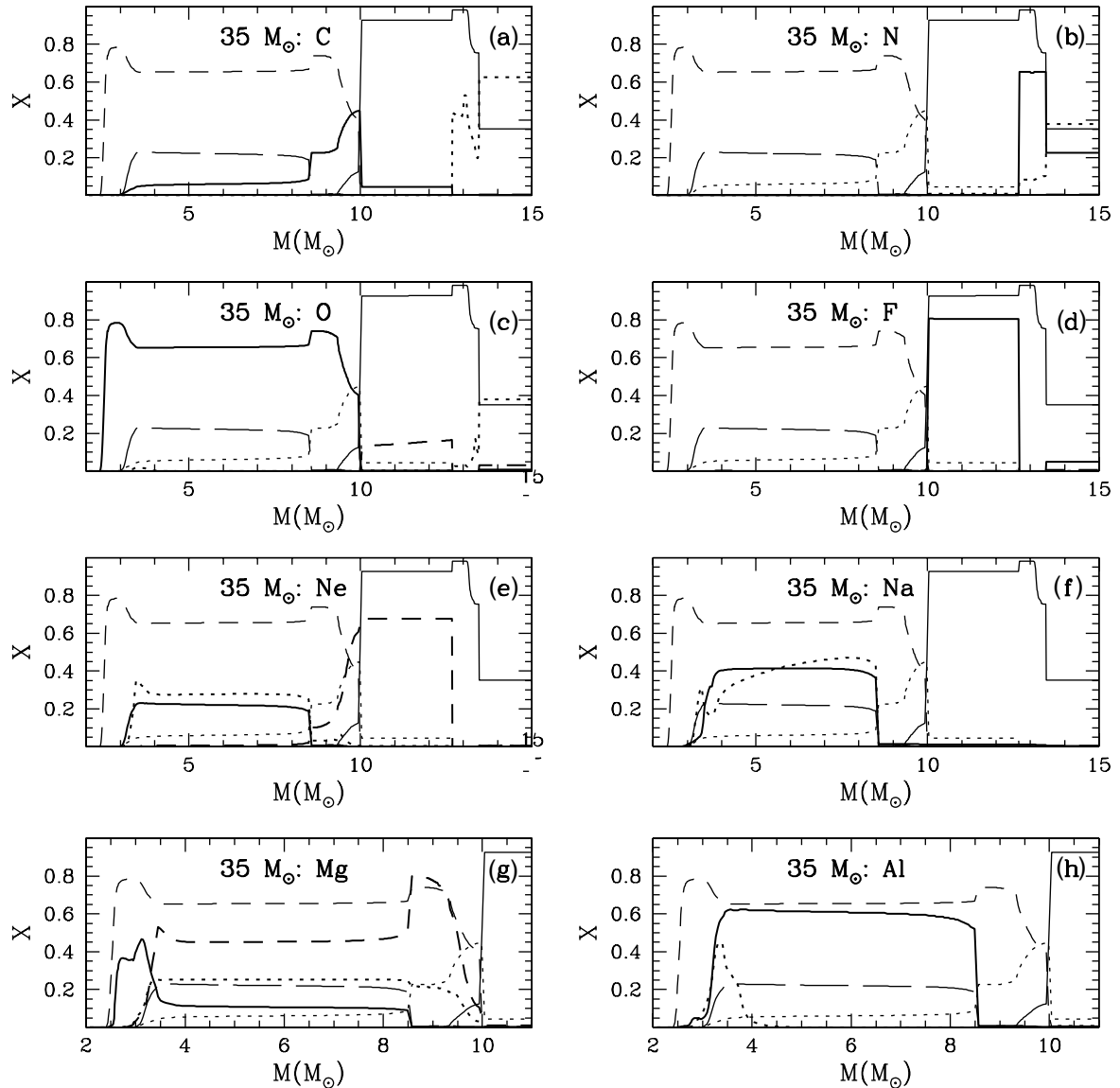


Figure 3 Same as Figure 1 but for the $35 M_{\odot}$ model.

convective shell is located far enough from the centre that no significant explosive burning occurs any more. ^{22}Ne is the main outcome of the burning (at $T \simeq 150 \times 10^6$ K) of the ^{14}N (produced by the CNO cycle in the H burning) by the sequence $^{14}\text{N}(\alpha, \gamma)^{18}\text{F}(\beta^+)^{18}\text{O}(\alpha, \gamma)^{22}\text{Ne}$ and then destroyed at temperatures larger than 250×10^6 K by both the $^{22}\text{Ne}(\alpha, \gamma)^{26}\text{Mg}$ and the $^{22}\text{Ne}(\alpha, n)^{25}\text{Mg}$ processes. Hence the destruction of this isotope starts towards the end of the central He burning phase and then completes in C burning. The final profile of ^{22}Ne shows that this isotope is confined to the He convective shell and to the layers between the external border of the C convective shell and the base of the He shell. The explosive burning does not alter its final yield in the $25 M_{\odot}$ and $35 M_{\odot}$ models, while the explosive C burning partly contributes to the final yield in the $15 M_{\odot}$ model. It goes without saying that the full evolution of the star must be followed in order to compute the yields of all the Ne isotopes. ^{23}Na is mainly produced by both the C and Ne burning

and then destroyed by the oxygen burning. In C burning the abundance of ^{23}Na is controlled by the balance between the $^{12}\text{C}(^{12}\text{C}, p)^{23}\text{Na}$ and the $^{23}\text{Na}(p, \alpha)^{20}\text{Ne}$ reactions while in Ne burning it is determined by the (quasi) equilibrium between the $^{20}\text{Ne}(\alpha, p)^{23}\text{Na}$ process and its reverse $^{23}\text{Na}(p, \alpha)^{20}\text{Ne}$, the main leakage coming from the $^{23}\text{Na}(\alpha, p)^{26}\text{Mg}$ reaction. Since the ashes of the Ne burning are largely reprocessed by the O burning, the production site of this isotope remains the C convective shell. Once again the blast wave modifies significantly its pre-explosive profile in the less massive model while it only marginally depletes the ^{23}Na at the very base of the C convective shell in the two more massive models. The unstable and γ -emitter isotope ^{22}Na is synthesised in the C convective shell and its abundance is determined by the balance between the $^{21}\text{Ne}(p, \gamma)^{22}\text{Na}$ and the $^{22}\text{Na}(\beta^+)^{22}\text{Ne}$ processes. The shock wave alters significantly the yield of this isotope only in the $15 M_{\odot}$ model.

5 The Production of Mg and Al

Figures 1, 2, and 3 show the final profiles of ^{24}Mg (thick solid line), ^{25}Mg (thick dotted line), and ^{26}Mg (thick dashed line) in panel (g) and of ^{26}Al (thick dotted line) and ^{27}Al (thick solid line) in panel (h) for the three stellar models of 15, 25, and 35 M_{\odot} . The thin solid, dotted, and dashed lines show, as a reference, the final profiles of ^4He , ^{12}C , and ^{20}Ne respectively. ^{24}Mg is produced by both C and Ne burning via the $^{20}\text{Ne}(\alpha, \gamma)^{24}\text{Mg}$ reaction. Since the matter exposed to the Ne burning is largely reprocessed by the O burning (that destroys this isotope), the final hydrostatic abundance of ^{24}Mg is the one produced by the C convective shell. In addition to the hydrostatic production, ^{24}Mg is also significantly produced (in all three masses) by the explosive Ne burning. Actually the production of ^{24}Mg in the 15 M_{\odot} model is exclusively due to the explosive Ne burning. ^{25}Mg is produced by the $^{22}\text{Ne}(\alpha, n)^{25}\text{Mg}$ process both in the He and C burning phases and also by the $^{24}\text{Mg}(\text{p}, \gamma)^{25}\text{Al}(\beta^+)^{25}\text{Mg}$ sequence in C burning. It is mainly destroyed by $^{25}\text{Mg}(\text{n}, \gamma)^{26}\text{Mg}$ in He burning, by $^{25}\text{Mg}(\text{p}, \gamma)^{26}\text{Al}$ in C burning, and by $^{25}\text{Mg}(\alpha, \text{n})^{28}\text{Si}$ in Ne burning. Figures 2 and 3 clearly show that the relative contributions of the C convective shell and the central He burning to the final yields depend on the initial mass of the star: in the 25 M_{\odot} model the ^{25}Mg yield is dominated by the contribution from the C convective shell while in the 35 M_{\odot} model it is dominated by the contribution from the central He burning. The influence of the explosion is quite modest for both masses in the sense that a small fraction (a few per cent) of this isotope is destroyed by the passage of the shock wave at the base of the C convective shell. In the 15 M_{\odot} star, on the other hand, ^{25}Mg is mainly produced by the C and Ne explosive burning. ^{26}Mg is mainly produced by the C convective shell plus a minor contribution from the central He burning.

Its abundance in the C convective shell (and hence its final yield) is regulated by the balance between the two main processes that produce it, namely $^{26}\text{Al}(\beta^+)^{26}\text{Mg}$ and $^{23}\text{Na}(\alpha, \text{p})^{26}\text{Mg}$, and the main process that destroys it, namely $^{26}\text{Mg}(\text{p}, \gamma)^{27}\text{Al}$. Also in this case the explosion plays a minor role in the two more massive models (just destroying a little bit of this isotope at the base of the C convective shell) while it dominates the final yield in the 15 M_{\odot} model. ^{27}Al is also mainly produced by the C convective shell and its final abundance is regulated by the competition between its production through the $^{26}\text{Mg}(\text{p}, \gamma)^{27}\text{Al}$ process and its destruction that occurs through two concurrent processes, namely the $^{27}\text{Al}(\text{n}, \gamma)^{28}\text{Al}$ and the $^{27}\text{Al}(\text{p}, \gamma)^{28}\text{Si}$ processes. Also in this case the explosive burning modifies significantly the yield of this isotope only in the 15 M_{\odot} model. The unstable and γ -emitter isotope ^{26}Al is initially produced and then progressively destroyed in the central H burning. The receding convective core leaves behind a peak of ^{26}Al that is then partly brought to the surface of the star by the first dredge-up. The yield of this isotope, however, fully comes from the C explosive burning that produces ^{26}Al in the region where the peak temperature of the shock front drops to $\simeq 2 \times 10^9$ K.

Acknowledgments

We warmly thank John Lattanzio and Brad Gibson for their kind hospitality in Melbourne.

References

- Limongi, M., & Chieffi, A. 2003, *ApJ*, 592, in press
- Rauscher, T., Heger, A., Hoffman, R.D., & Woosley, S. E. 2002, *ApJ*, 576, 323
- Woosley, S. E., & Weaver, T. A. 1995, *ApJS*, 101, 181